Bull. Mater. Sci., Vol. 31, No. 7, December 2008, pp. 1007–1013. © Indian Academy of Sciences.

Nonlinear electrical properties and aging characteristics of (NiO, MgO, Cr_2O_3)-doped Zn–Pr–Co–R (R = Y, Er) oxide-based varistors

CHOON-W NAHM

Semiconductor Ceramics Laboratory, Department of Electrical Engineering, Dongeui University, Busan 614-714, Republic of Korea

MS received 19 April 2008; revised 12 August 2008

Abstract. The electrical properties and stability of the varistors, which composed of (NiO, MgO, Cr_2O_3)-doped Zn–Pr–Co–R (Y, Er) oxide-based ceramics, were investigated for different additives. The breakdown voltage of the varistors increased in order of NiO→undoped→MgO→Cr_2O_3: 1200→1551→1691→1959 V/cm for ZPCY system and undoped→NiO→MgO→Cr_2O_3: 1024→1041→1500→1668 V/cm for ZPCE system, respectively. The nonlinear coefficient value increased in order of undoped→NiO→MgO→Cr_2O_3: 21→25→38→50 in ZPCY system and NiO→undoped→MgO→Cr_2O_3: 27→32→35→38 in ZPCE system, respectively. In ZPCY and ZPCE systems, the Cr_2O_3-additives most greatly improved the nonlinear properties. In Cr_2O_3-doped system, ZPCY system exhibited higher nonlinear properties than that of ZPCE system. The stability against d.c. accelerated aging stress was higher in Cr_2O_3-additives than in NiO- and MgO-additives for ZPCY system and was higher in NiO-additives than in MgO- and Cr_2O_3-additives for ZPCE system.

Keywords. ZnO; varistors; microstructure; nonlinear electrical properties; aging characteristics.

1. Introduction

ZnO varistors are electroceramic semiconductor devices made by sintering ZnO powder doped with minor additives, such as Bi_2O_3, Pr_6O_{11}, CoO, and so on. Their electrical characteristics are basically related to the grain boundary in bulk of the devices. Each ZnO grain acts as if it has a semiconductor junction at the grain boundary.

Since nonlinear electrical behaviour occurs at a boundary of each semiconducting ZnO grain, the varistors can be considered as a multi-junction device composed of many series and parallel connection of grain boundaries. The grain size distribution plays a major role in electrical behaviour. ZnO varistors exhibit highly nonlinear voltage–current (V–I) characteristics because of the electronic phenomena occurring near the grain boundaries. In other words, they exhibit high impedance similar to insulator below the varistor voltage, called the breakdown voltage, and very low impedance similar to conductor thereafter. Moreover, they possess excellent surge withstanding capability. Therefore, they have been widely utilized as the surge absorbers in electronic system and the core elements of surge arresters in electric power system (Levison and Phillip 1986; Gupta 1990).

The majority of commercial varistors are Bi-based ZnO varistors containing Bi_2O_3, which inherently induces nonlinear properties. However, they possess a few drawbacks (Lee and Tseng 1992) caused by high volatility and reactivity of Bi_2O_3. In recent years, Pr-doped ZnO varistors have been studied to overcome these problems (Alles and Burdick 1991; Lee *et al* 1996; Chun *et al* 1999; Nahm *et al* 2000; Chun and Mizutani 2001). Nahm *et al* reported that the ternary system ZnO–Pr_6O_{11}–CoO-based varistors have highly nonlinear properties when rare earth metal oxides, R_2O_3 (R = Er, Dy, Nd) are doped (Nahm *et al* 2000; Nahm 2003). To develop the varistors of high performance, it is very important to comprehend the effects of the individual additives on varistor characteristics. NiO, MgO, and Cr_2O_3 are subordinate additives, and one or two of them is usually doped to the varistor composition. However, no roles of them have been compared in Bi_2O_3 and Pr_6O_{11}-based varistors, reported previously.

This paper is to investigate the influence of additives (NiO, MgO, Cr_2O_3) on microstructure, nonlinear electrical properties, and stability of quaternary system ZnO–Pr_6O_{11}–CoO–Y_2O_3-based varistors (in short, ZPCY system) and ZnO–Pr_6O_{11}–CoO–Er_2O_3-based varistors (in short, ZPCE system).

2. Experimental

2.1 *Sample preparation*

Reagent-grade raw materials were used in proportions of 97·5 mol% ZnO, 0·5 mol% Pr_6O_{11}, 1 mol% CoO, 0·5 mol% (Y_2O_3, Er_2O_3, independently), 0·5 mol% (Ni, Mg, Cr oxide,

(cwnahm@deu.ac.kr)

independently). Raw materials were mixed by ball milling with zirconia balls and acetone in a polypropylene bottle for 24 h. The mixture was dried at 120°C for 12 h and calcined in air at 750°C for 2 h. The calcined mixture was pulverized using an agate mortar/pestle and after 2 wt% polyvinyl alcohol (PVA) binder addition, granulated by sieving through a 100-mesh screen to produce the starting power. The power was uniaxially pressed into discs of 10 mm in diameter and 2 mm in thickness at a pressure of 80 MPa. The discs were sintered at 1350°C in air for 1 h and furnace-cooled to room temperature. The heating and cooling rates were 4°C/min. The sintered samples were lapped and polished to 1 mm thickness. The final samples were about 8 mm in diameter and 1 mm in thickness. Silver paste was coated on both faces of samples and the silver electrodes were formed by heating at 600°C for 10 min. The electrodes were 5 mm in diameter.

2.2 *Microstructure measurement*

Both surfaces of the samples were lapped and ground with SiC paper and polished with Al_2O_3 powder to a mirror-like surface. The polished samples were thermally etched at 1100°C for 30 min. The surface microstructure was examined by a scanning electron microscope (SEM, Hitachi S2400, Japan). The average grain size (d) was determined by the linear intercept method such as the following equation (Wurst and Nelson 1972):

$$d = 1{\cdot}56L/MN,$$

where L is the random line length on the micrograph, M the magnification of the micrograph, and N the number of the grain boundaries intercepted by lines. The sintered density (ρ) was measured using a density determination kit (238490) attached to balance (Mettler, AG 245) by the Archimedes method.

2.3 *E–J characteristics measurement*

The electric field–current density (E–J) characteristics were measured using a high voltage source/measure unit (Keithley 237). The breakdown field ($E_{1\ mA}$) was measured at 1 mA·cm^{-2} and the leakage current density (J_L) was defined as the current at 0·80 $E_{1\ mA}$. In addition, the non-ohmic coefficient (α) is defined by the empirical law, $J = K{\cdot}E^{\alpha}$, where J is the current density, E the applied electric field, and K a constant. α was determined in the current density range of 1 mA/cm^2 to 10 mA/cm^2, where $\alpha = 1/(\log E_2 - \log E_1)$, and E_1 and E_2 are the electric field corresponding to 1 mA/cm^2 and 10 mA/cm^2, respectively.

2.4 *D.C. accelerated aging characteristics measurement*

The stability against d.c. accelerated aging stress was performed under four continuous states; (i) the 1st stress: 0·85 $E_{1\ mA}$/115°C/24 h, (ii) the 2nd stress: 0·90 $E_{1\ mA}$/120°C/24 h, (iii) the 3rd stress: 0·95 $E_{1\ mA}$/125°C/24 h and (iv) the 4th stress: 0·95 $E_{1\ mA}$/150°C/24 h.

Simultaneously, the leakage current during the stress time was monitored at intervals of 1 min by a high voltage source-measure unit (Keithley 237). The varistors stressed were applied to the electrical characteristics after storage at normal room temperature for 2 h. The degradation rate coefficient (K_T) was calculated from the following equation (Fan and Freer 1994):

$$I_L = I_{Lo} + K_T t^{1/2},$$

where I_L is the leakage current at stress time (t) and I_{Lo} is I_L at $t = 0$. After the respective stresses, the E–J characteristics were measured at room temperature. Five samples were used for all electrical measurements and their average value is presented.

3. Results and discussion

SEM micrographs of the ZPCY and ZPCE system doped with different additives are shown in figures 1 and 2, respectively. It can be seen that the microstructure is very simple having only two phases regardless of additives: ZnO grain (bulk phase) and intergranular layer (second phase). It is well known that this is one of the important features in Pr-based ZnO varistors (Mukae 1987). The intergranular layers in varistors were Pr- and Y-rich phases in figure 1 and Pr- and Er-rich phases in figure 2, generated by segregating due to large ionic radius compared with Zn^{2+}. The sintered density decreased in order of NiO→undoped→MgO→Cr_2O_3: 5·59→5·55→5·39→5·34 g/cm^3 in ZPCY system and undoped→NiO→Cr_2O_3→MgO: 5·69→5·68→5·58→5·50 g/cm^3 in ZPCE system. The NiO-additives increased the density in ZPCY system, whereas scarcely affected the density in ZPCE system. The MgO- and Cr_2O_3-additives greatly decreased the density in all systems. The average grain size decreased in order of NiO→undoped→MgO→Cr_2O_3: 17·5→13·7→13·6→11·4 μm in ZPCY system and NiO→MgO→undoped→Cr_2O_3: 18·6→15·8→15·7→14·2 μm in ZPCE system. The detailed microstructural parameters are shown in tables 1 and 2.

The conduction characteristics of the ZPCY and ZPCE system doped with different additives are shown in figures 3 and 4, respectively. The varistors show conduction characteristics divided into two regions: pre-breakdown at low field and breakdown at high field. The sharper the knee of the curves between the two regions, the better the nonlinear properties. It can be forecasted that ZPCY and ZPCE system doped with Cr_2O_3-additives should exhibit the best nonlinear properties because it has the sharpest knee. For remainder additives, the knee becomes less pronounced and is close to found shape. The detailed V–I parameters are shown in tables 1 and 2.

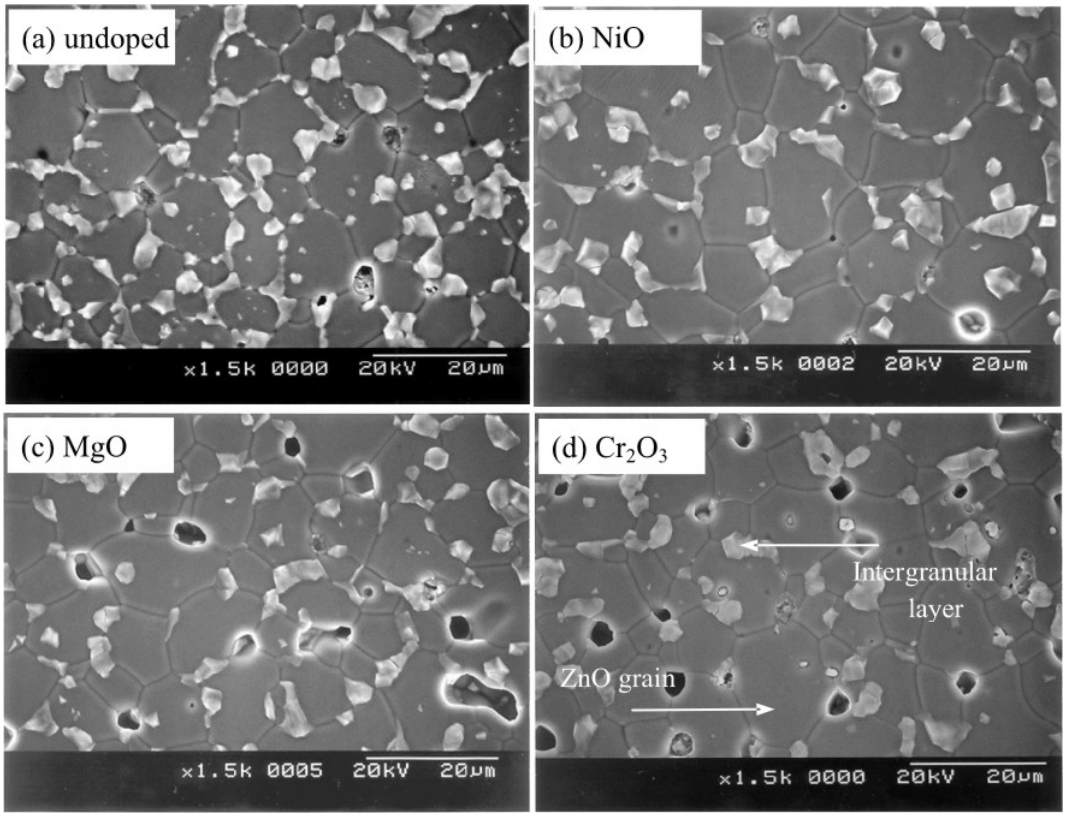

Figure 1. SEM micrograph of ZPCY system for different additives.

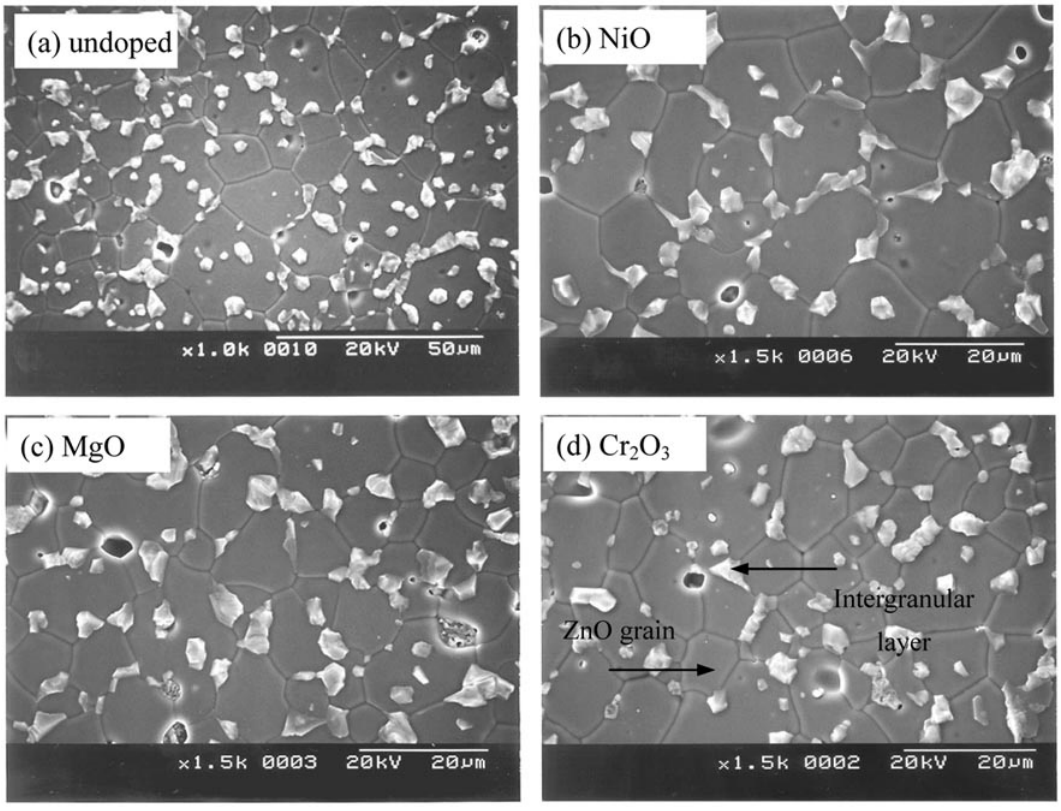

Figure 2. SEM micrograph of ZPCE system for different additives.

The breakdown field (E_{1mA}) increased in order of NiO→undoped→MgO→Cr_2O_3: 200→1551→1691→1959 V/cm in ZPCY system and undoped→NiO→MgO→Cr_2O_3: 1024→1041→1500→1668 V/cm in ZPCE system. It can be seen that this is attributed to the decrease in the number of grain boundaries caused by the decrease in the ZnO grain size. The α value increased in order of undoped→NiO→MgO→Cr_2O_3: 21·3→25·2→37·9→50·2 in ZPCY system and NiO→undoped→MgO→Cr_2O_3: 27·0→31·8→35·1→38·1 in ZPCE system. In ZPCY system, all additives improved the nonlinear properties. On the contrary, in ZPCE system, only NiO-additives deteriorated nonlinear properties. MgO- and Cr_2O_3-additives greatly increased the nonlinear properties in all systems. This shows that the selection of additives is very important. On the other hand, the I_L value greatly decreased in order of NiO→undoped→MgO→Cr_2O_3: 77·0→48·5→40·8→8·2 μA/cm^2 in ZPCY system and NiO→MgO→undoped→Cr_2O_3: 80·6→49·5→33·2→12·2 μA/cm^2 in ZPCE system. It can be seen that the variation of J_L value shows the inverse relationship to the variation of α value. Therefore, it was confirmed that the nonlinear properties are strongly influenced by the additives.

In application of varistors, one of the important factors that should be necessarily considered is the stability of nonlinear properties. The electronic and electrical system to be protected from various surges significantly requires a high stability of varistors above all in order to enhance their reliability. In practice, ZnO varistors begin to degrade because of gradually increasing leakage current with stress time. Eventually, they loose a varistor function due to the thermal runaway. In this viewpoint, in addition to nonlinearity, the electrical stability is technologically very important characteristic of ZnO varistors. In general, the allowed specifications of $\%\Delta E_{1\,mA}$ for the commercial varistors are less than 10% under 0·85 $E_{1\,mA}$/85°C/1000 h. Even though the stressing time in this study is short, the stressing voltage and ambient temperature are very severe.

The variations of the leakage current of the varistor doped with different additives during d.c. accelerated aging stress are shown in figures 5 and 6. Undoped-, NiO- and MgO-doped ZPCY system exhibited a high stability until the third stress (0·95 $E_{1\,mA}$/125°C/24 h), whereas the thermal runaway within a short time, under the fourth stress (0·95 $E_{1\,mA}$/150°C/24 h). The stability for varistors can be estimated by the degradation rate coefficient (K_T), indicating the degree of aging. The lower the K_T value, the higher the stability. It can be seen that NiO- and MgO-doped ZPCY system greatly improved the stability because they exhibited much lower K_T than the undoped system. On the contrary, the Cr_2O_3-doped ZPCY system exhibited a high stability without thermal runaway until the fourth stress. However, these systems exhibited posi-

Table 1. Microstructural and *E–J* characteristic parameters of ZPCY system for different additives.

System	Additives	ρ (g/cm^3)	d (μm)	$E_{1\,mA}$ (V/cm)	α	J_L (μA/cm^2)
ZPCY	Undoped	5·55	13·7	1551	21·3	48·5
	NiO	5·59	17·5	1200	25·2	77·0
	MgO	5·39	13·6	1691	37·9	40·8
	Cr_2O_3	5·34	11·4	1959	50·2	8·2

Table 2. Microstructural and *E–J* characteristic parameters of ZPCE system for different additives.

System	Additives	ρ (g/cm^3)	d (μm)	$E_{1\,mA}$ (V/cm)	α	J_L (μA/cm^2)
ZPCE	Undoped	5·69	15·7	1024	31·8	33·2
	NiO	5·68	18·6	1041	27·0	80·6
	MgO	5·50	15·8	1500	35·1	49·5
	Cr_2O_3	5·58	14·2	1640	38·1	12·2

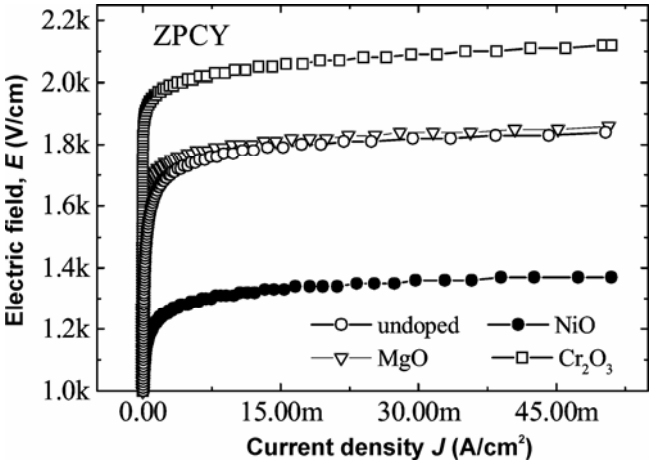

Figure 3. *E–J* characteristics of ZPCY system for different additives.

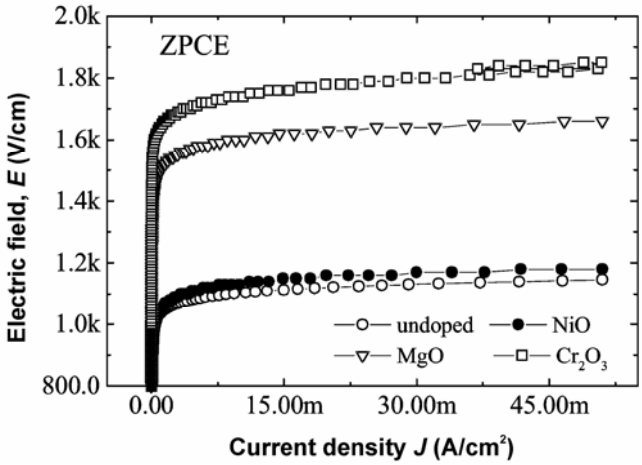

Figure 4. *E–J* characteristics of ZPCE system for different additives.

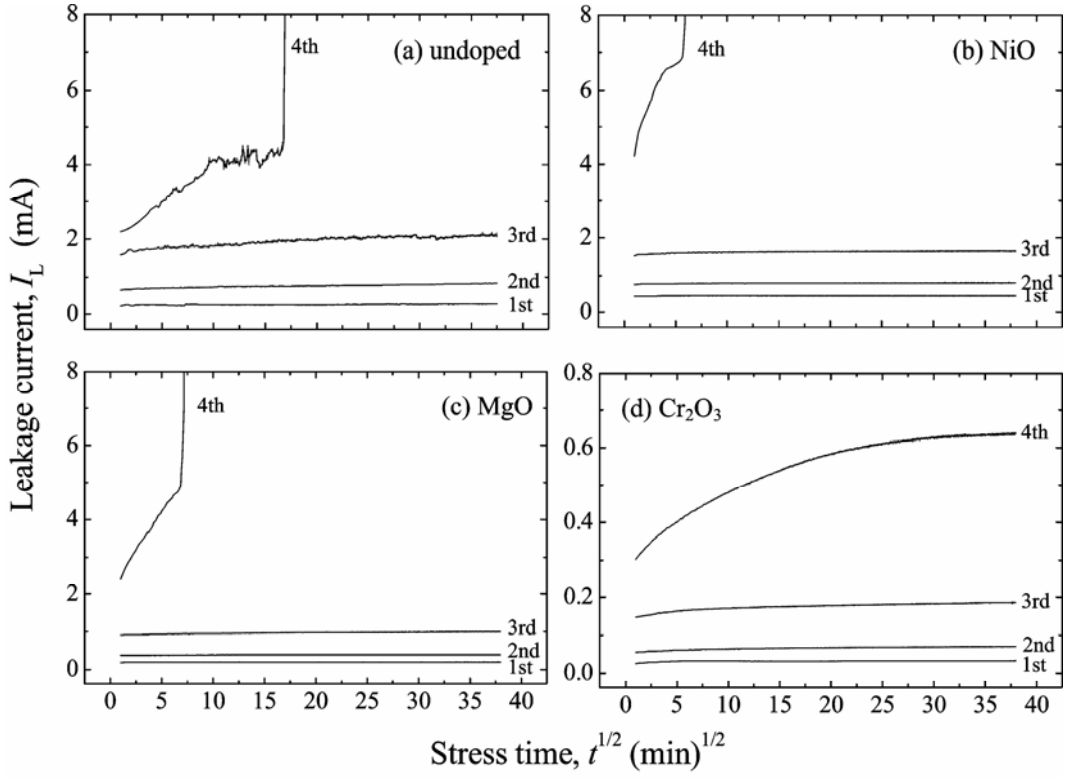

Figure 5. Variation of leakage current during d.c. accelerated aging stress of ZPCY system for different additives.

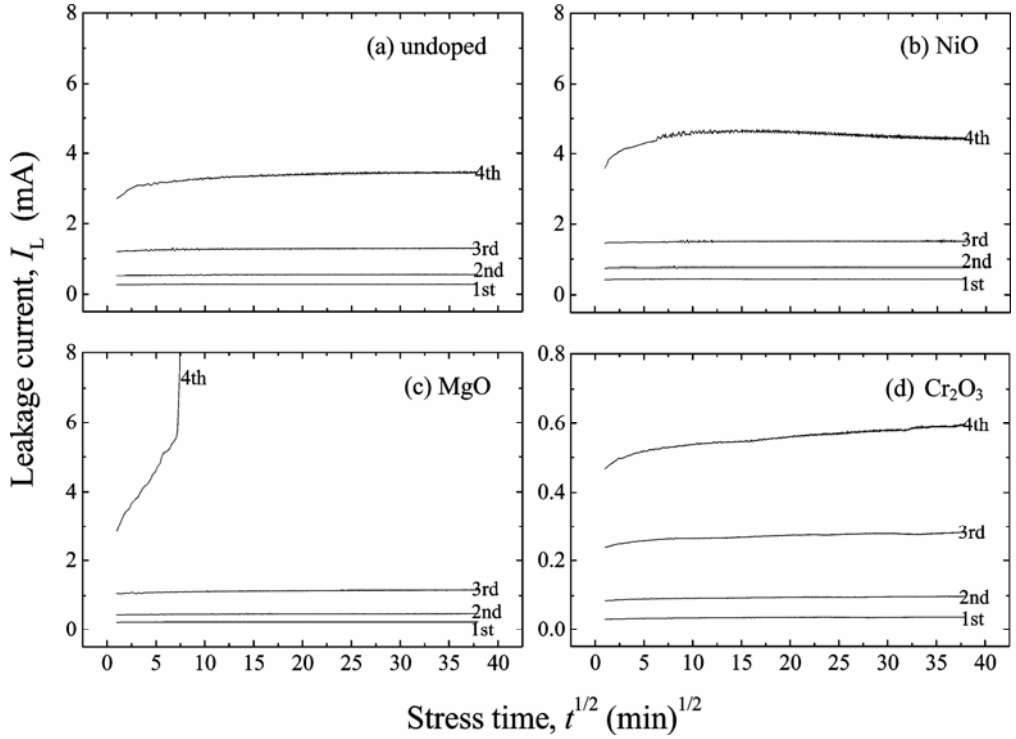

Figure 6. Variation of leakage current during d.c. accelerated aging stress of ZPCE system for different additives.

Table 3. Variation of E–J characteristic parameters after d.c. accelerated aging stress of ZPCY system for different additives.

System	Additives	Stress state	K_T ($\mu A \cdot h^{-1/2}$)	$E_{1\,mA}$ (V/cm)	$\%\Delta E_{1\,mA}$	α	$\%\Delta\alpha$	J_L ($\mu A/cm^2$)	$\%\Delta J_L$
ZPCY	Undoped	Before	–	1551		21·3		48·5	
		1st	8·9	1532	–1·2	19·7	–7·5	68·4	41·0
		2nd	28·4	1510	–2·6	18·9	–11·3	77·0	58·8
		3rd	58·9	1500	–3·3	17·9	–16·0	103·1	112·6
		4th			Thermal runaway				
	NiO	Before	–	1200	0	25·2	0	77·0	0
		1st	–0·5	1193	0·6	26·4	4·8	68·4	–11·2
		2nd	3·1	1190	–0·8	26·1	3·6	71·4	–7·3
		3rd	6·9	1187	–1·1	25·8	2·4	78·1	1·4
		4th			Thermal runaway				
	MgO	Before	–	1691	0	37·9	0	40·8	0
		1st	0·4	1686	–0·3	39·6	4·5	27·6	–32·4
		2nd	1·8	1682	–0·5	38·7	2·1	37·8	–7·4
		3rd	9·5	1676	–0·9	36·8	–2·9	69·9	71·3
		4th			Thermal runaway				
	Cr_2O_3	Before	–	1959	0	50·2	0	8·2	0
		1st	0·4	1937	–1·1	50·8	1·2	25·5	211·0
		2nd	1·5	1953	–0·3	48·7	–3·0	37·2	353·7
		3rd	3·8	1949	–0·5	47·2	–6·0	57·1	596·3
		4th	34·7	1895	–3·3	33·1	–34·1	301·0	3570·1

tive creep of leakage current (PCLC) through entire stress states, in which the K_T value was +0·4, +1·5, +3·8, and +34·7 $\mu A \cdot h^{-1/2}$, respectively, from the first to the fourth stress. In particular, it shows high K_T value in the fourth stress. The detailed parameters such as the variation rate of the breakdown field ($\%\Delta E_{1\,mA}$), variation rate of the nonlinear coefficient ($\%\Delta\alpha$), and variation rate of the leakage current density ($\%\Delta J_L$) after various d.c. accelerated aging stresses are shown in table 3.

As a result, the stability against d.c. accelerated aging stress in ZPCY system was slightly improved by NiO- and MgO-additives, whereas greatly improved by Cr_2O_3-additives. The stability in Cr_2O_3-doped ZPCY system marked $\%\Delta E_{1\,mA} = -3{\cdot}3\%$, $\%\Delta\alpha = -34{\cdot}1\%$ and $\%\Delta J_L = +3570{\cdot}1\%$ under the fourth stress (0·95 $E_{1\,mA}$/150°C/24 h).

On the other hand, the MgO-doped ZPCE system exhibited a high stability until the third stress, whereas the thermal runaway within a short time, under the fourth stress. However, undoped-, NiO-, and Cr_2O_3-doped ZPCE system exhibited a high stability without thermal runaway until the fourth stress. The Cr_2O_3-doped ZPCE system exhibited positive creep of leakage current (PCLC) through entire stress states, in which the K_T value was +0·4, +1·4, +4·0, and +15·5 $\mu A \cdot h^{-1/2}$, respectively from the first to the fourth stress. On the contrary, the NiO-doped ZPCE system exhibited negative creep of leakage current (NCLC) through entire stress states, in which the K_T value was –2·5, –0·5, +0·6 and –74·4 $\mu A\ h^{-1/2}$, respectively, from the first to the fourth stress. As a result, it can be seen that NiO-doped ZPCE system exhibited high stability, which is a rare case in the varistors. The detailed parameters such as $\%\Delta E_{1\,mA}$, $\%\Delta\alpha$ and $\%\Delta J_L$ after various d.c. accelerated aging stresses are shown in table 4.

As a result, the stability against d.c. accelerated aging stress in ZPCE system was greatly improved by NiO-additives, whereas greatly deteriorated by MgO-additives. The stability in NiO-doped ZPCE system marked $\%\Delta E_{1\,mA} = -1{\cdot}2\%$, $\%\Delta\alpha = -1{\cdot}1\%$, and $\%\Delta J_L = +9{\cdot}6\%$ under the fourth stress (0·95 $E_{1\,mA}$/150°C/24 h). Overall, ZPCE system with additives exhibited higher stability than ZPCY system. This can be explained as follows. The low sintered density and high leakage current greatly decrease the resistance for the stability. The former decreases the number of conduction path and eventually leads to the concentration of current. The latter leads to repetition cycle between joule heating and leakage current.

The leakage current of ZPCE system with additives is high compared with that of ZPCY system. On the contrary, the sintered density of ZPCE system with additives is high compared with that of ZPCY system. As considering two factors, in the light of the stability of ZPCE system > ZPCY system, it is assumed that the sintered density more greatly affects than the leakage current. Compared with NiO- and Cr_2O_3-doped ZPCE system, the sintered density of NiO-doped ZPCE system is larger than that of Cr_2O_3-doped ZPCE system and the leakage current of Cr_2O_3-doped ZPCE system is much lower than that of NiO-doped ZPCE system. In view of stability, it was also confirmed that the sintered density more greatly affects than the leakage current. Furthermore, the Cr_2O_3-doped ZPCE system exhibited larger variation of characteristics than undoped ZPCE system.

It is assumed that presumably the increase or decrease of the varistor characteristics in order of NiO→MgO→Cr_2O_3 relates to ionic radius of additives, which decreases in order of 0·72→0·66→0·64 Å. In discussing stability, the model for stability according to various stresses is

Table 4. Variation of E–J characteristic parameters after d.c. accelerated aging stress of ZPCE system for different additives.

System	Additives	Stress state	K_T (μA·h$^{-1/2}$)	$E_{1\,mA}$ (V/cm)	$\%\Delta E_{1\,mA}$	α	$\%\Delta\alpha$	J_L (μA/cm^2)	$\%\Delta J_L$
ZPCE	Undoped	Before	–	1024	0	31·8	0	33·2	0
		1st	0·26	1017	–0·7	30·8	–3·1	36·2	9·0
		2nd	2·46	1015	–0·9	30·5	–4·1	37·8	13·9
		3rd	8·37	1011	–1·3	29·8	–6·3	42·3	27·4
		4th	53·91	1003	–2·1	28·9	–9·1	54·1	63·0
	NiO	Before	–	1041	0	27·0	0	80·6	0
		1st	–2·49	1036	–0·5	28·0	3·6	70·9	–12·0
		2nd	–0·50	1036	–0·5	28·0	3·7	71·4	–11·4
		3rd	0·62	1034	–0·7	27·6	2·3	75·5	–6·3
		4th	–74·44	1029	–1·2	26·7	–1·1	88·3	9·6
	MgO	Before	–	1500	0	35·1	0	49·5	0
		1st	0·33	1491	–0·6	36·1	2·9	34·2	–30·9
		2nd	2·98	1489	–0·8	35·7	1·7	44·4	–10·3
		3rd	12·08	1482	–1·2	33·9	–3·6	82·1	65·9
		4th			Thermal runaway				
	Cr_2O_3	Before	–	1640	0	38·1	0	12·2	0
		1st	0·43	1625	–0·9	35·9	–5·8	15·3	25·4
		2nd	1·36	1617	–1·4	35·1	–7·9	22·9	87·7
		3rd	4·00	1604	–2·2	33·2	–12·8	30·6	150·8
		4th	15·49	1597	–2·6	30·5	–19·9	59·7	389·3

known to be ion migration mechanism proposed by Gupta and Carlson (Gupta 1985). According to this, when ZnO varistors are stressed continuously by an electric field, the positively charged zinc interstitial (Zn_i) formed and frozen in the depletion layer, during cooling from sintering temperature, migrates toward the negatively charged grain boundary interface, and it recombines with zinc vacancy (V_{Zn}) positioned there. As a result, the recombination of these species gives rise to a lowering of the potential barrier at the grain boundaries and leads to the degradation of ZnO varistors. In the light of these facts, it is guessed that the reason why the additives affect the stability is deeply related to the migration of zinc interstitial (Zn_i) within a depletion layer or the stabilization of the interface states. In present status, this is unclear, whereas it should be studied in the future.

4. Conclusions

The nonlinear electrical properties and stability against d.c. accelerated aging stress of the ZPCY system and ZPCE system were investigated for different additives (NiO, MgO, Cr_2O_3). The nonlinear properties of both systems were gradually improved in order of NiO→MgO→Cr_2O_3. The NiO- and MgO-doped systems were nearly equal in nonlinear coefficient, whereas in Cr_2O_3-doped system, ZPCY system exhibited much higher than ZPCE system in nonlinear coefficient. In stability against d.c. accelerated aging stress, NiO-doped ZPCE system and Cr_2O_3-doped ZPCY system exhibited a higher stability compared with other systems. Overall, ZPCE system was found to be higher than ZPCY system for stability against d.c. accelerated aging stress.

References

Alles A B and Burdick V L 1991 *J. Appl. Phys.* **70** 6883

Chun S Y and Mizutani N 2001 *Mater. Sci. Eng.* **B79** 1

Chun S Y, Shinozaki K and Mizutani N 1999 *J. Am. Ceram. Soc.* **82** 3065

Fan J and Freer R 1994 *J. Am. Ceram. Soc.* **77** 2663

Gupta T K 1990 *J. Am. Ceram. Soc.* **73** 1817

Gupta T K and Carlson W G 1985 *J. Mater. Sci.* **20** 3487

Lee Y S and Tseng T Y 1992 *J. Am. Ceram. Soc.* **75** 1636

Lee Y S, Liao K S and Tseng T Y 1996 *J. Am. Ceram. Soc.* **79** 2379

Levinson L M and Philipp H R 1986 *Am. Ceram. Soc. Bull.* **65** 639

Mukae K 1987 *Am. Ceram. Soc. Bull.* **66** 1329

Nahm C W 2003 *Solid State Commun.* **126** 281

Nahm C W, Park C H and Yoon H S 2000 *J. Mater. Sci. Lett.* **19** 271, 725

Wurst J C and Nelson J A 1972 *J. Am. Ceram. Soc.* **55** 109